



Vibrational frequencies and infrared intensities of the hydrogen-bonded complexes of nitrous acid with ethers: ab initio and DFT studies

Yordanka Dimitrova*, Iva Slavova

Institute of Organic Chemistry, Bulgarian Academy of Sciences, Acad. G. Bonchev Str., 1113 Sofia, Bulgaria

Received 1 July 2004; accepted 27 July 2004

Abstract

The vibrational spectra of the binary complexes formed by HONO-*trans* and HONO-*cis* with dimethyl and diethyl ethers have been investigated using ab initio calculations at the SCF and MP2 levels with 6-311++G(d,p) basis set and B3LYP calculations with 6-31G(d,p) and 6-31+G(d,p) basis sets. Full geometry optimisation was made for the complexes studied. The accuracy of the ab initio calculations have been estimated by comparison between the predicted values of the vibrational characteristics (vibrational frequencies and infrared intensities) and the available experimental data. It was established, that the methods, used in this study are well adapted to the problem under examination. The predicted values with the B3LYP calculations are very near to the results, obtained with 6-311++G(d,p)/MP2. The ab initio and DFT calculations show that the changes in the vibrational characteristics (vibrational frequencies and infrared intensities) upon hydrogen bonding for the hydrogen-bonded complex $(\text{CH}_3)_2\text{O} \cdots \text{HONO-}trans$ are larger than for the complex $(\text{CH}_3)_2\text{O} \cdots \text{HONO-}cis$.

© 2004 Elsevier B.V. All rights reserved.

Keywords: Hydrogen bonding; Nitrous acid; Ab initio and DFT calculations; Vibrational spectra

1. Introduction

Nitrous acid plays an important role in atmospheric chemistry, forming hydrogen-bonded complexes with number of atmospheric bases and is one of the smallest molecules, which exhibits a *cis-trans* conformational equilibrium. The direct measurements of the rates and mechanisms of heterogeneous reactions on surfaces or in liquid droplets are hard to carry out under the conditions of the Antarctic stratosphere. In this connection, the computer simulations of such reactions are very useful for the clarification of the structure and stability of the hydrogen-bonded complexes important for atmospheric chemistry [1–10].

Weakly bound molecular complexes have been extensively investigated in the gas phase by radiofrequency, microwave, and high-resolution infrared spectroscopy [11]. The matrix infrared spectra provide very common information about the hydrogen bonding and structure of such systems

[12]. The infrared matrix isolation studies on the complexes of nitrous acid with important atmospheric species: N₂, CO [13], NH₃ [14], CH₄, C₂H₂ [15] and oxygen bases (acetone and ethers) [16] have been reported. The interaction between nitrous acid and atmospheric species is of potential interest in connection with atmospheric modelling. Nitrous acid is unstable in the gas phase and occurs in complex equilibrium with the product of its decomposition [17].

Dimethyl and diethyl ethers have been widely used as oxygen bases in the studies of hydrogen bonding. Barnes and Wright [18] have been reported the studies in argon and nitrogen matrices of the complexes of dimethyl and diethyl ethers with hydrogen halides.

The aim of the present study is to investigate the changes in the vibrational characteristics (vibrational frequencies and infrared intensities) arising from the hydrogen bonding between *trans*- and *cis*-HONO and ethers (dimethyl and diethyl). The ab initio calculations at the SCF and MP2 levels with 6-311++G(d,p) basis sets and DFT calculations (B3LYP/6-31G(d,p) and B3LYP/6-31+G(d,p)) have been performed for the complexes studied.

* Corresponding author. Fax: +359 2 931 0018.

E-mail address: dimj@orgchm.bas.bg (Y. Dimitrova).

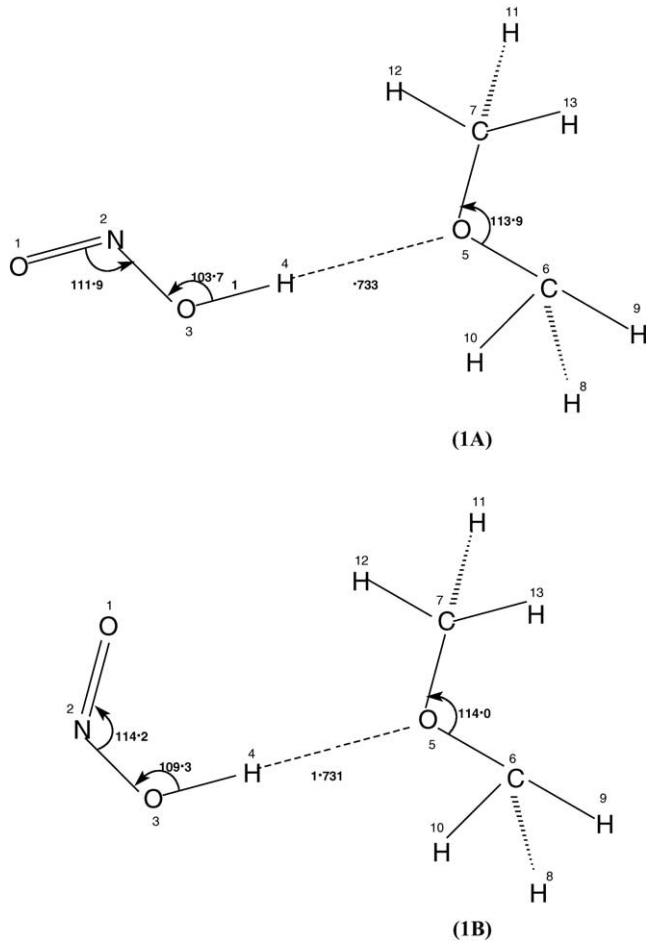


Fig. 1. Optimized structures with the B3LYP/6-31+G(d,p) calculations and atomic numbering for the hydrogen-bonded complexes: $(\text{CH}_3)_2\text{O} \cdots \text{HONO-}trans$ (**1A**) and $(\text{CH}_3)_2\text{O} \cdots \text{HONO-}cis$ (**1B**).

2. Results and discussion

2.1. Structures and stability

In order to establish the most stable structures for the complexes of dimethyl and diethyl ethers with HONO (*trans* and *cis*) ab initio calculations at SCF and MP2 levels and B3LYP calculations have been performed using the GAUSSIAN 98 series of programs [19]. Our aim was to select the most stable structures for the complexes studied: $(\text{CH}_3)_2\text{O} \cdots \text{HONO-}trans$ (**1A**), $(\text{CH}_3)_2\text{O} \cdots \text{HONO-}cis$ (**1B**), $(\text{C}_2\text{H}_5)_2\text{O} \cdots \text{HONO-}trans$ (**2A**), $(\text{C}_2\text{H}_5)_2\text{O} \cdots \text{HONO-}cis$ (**2B**). In Figs. 1 and 2 and Table 1 are shown the structures, optimum values of the total energy and optimised structural parameters for the hydrogen-bonded complexes **1A**, **1B** and **2A**, **2B**. As can be seen from the results of the E^{tot} in Table 1, the *trans*-complexes **1A** and **2A** are more stable than the *cis*-complexes **1B** and **2B**. The comparison between the bond lengths and angles for the binary complexes and those for the monomers show that as a result of the hydrogen bonding their values are slightly perturbed.

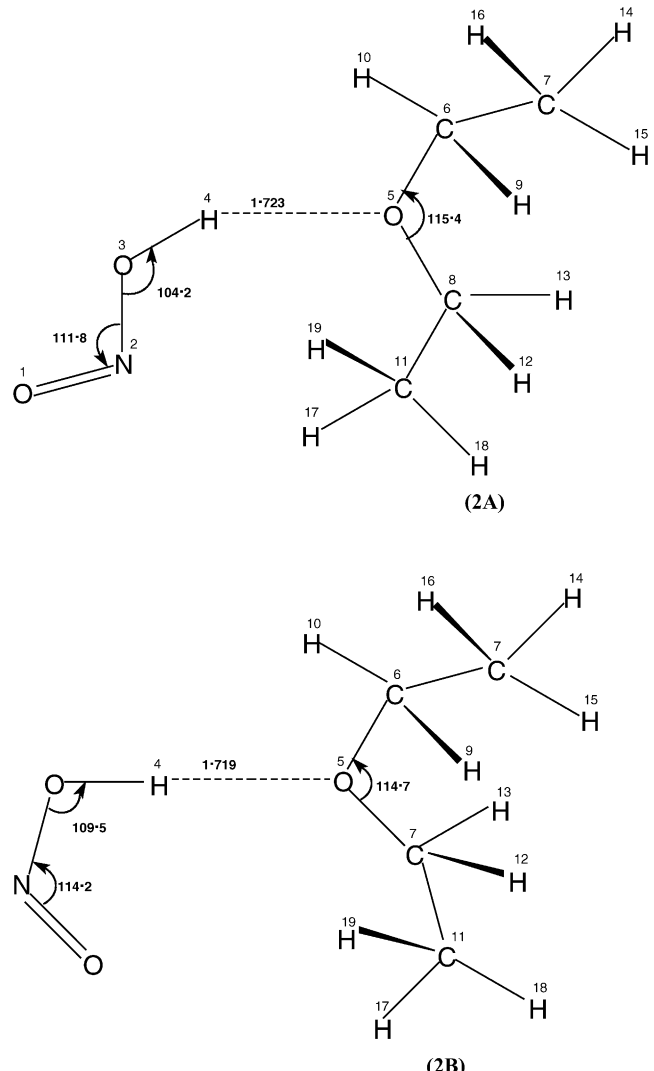


Fig. 2. Optimized structures with the B3LYP/6-31+G(d,p) calculations and atomic numbering for the hydrogen-bonded complexes: $(\text{C}_2\text{H}_5)_2\text{O} \cdots \text{HONO-}trans$ (**2A**) and $(\text{C}_2\text{H}_5)_2\text{O} \cdots \text{HONO-}cis$ (**2B**).

The dissociation energy (uncorrected and BSSE-corrected) for the complexes **1A**, **1B**, **2A** and **2B** was calculated in order to estimate the stability of the complexes. As can be seen from the results in Table 2, the *trans*-complexes **1A** and **2A** are more stable than the *cis*-complexes **1B** and **2B**. Having in mind the corrected values of the dissociation energy for the complexes of dimethyl and diethyl ethers with HONO (*trans* and *cis*) it can be concluded that these complexes have very near stability.

2.2. Vibrational frequencies and infrared intensities

The vibrational frequencies and infrared intensities for free monomers (HONO-*trans*, HONO-*cis* and $(\text{CH}_3)_2\text{O}$) and for the binary complexes **1A** and **1B** (see Fig. 1) have been predicted by ab initio calculations at the SCF and MP2 levels

Table 1

Selected geometric parameters for free and complexed HONO, $(\text{CH}_3)_2\text{O}$ and $(\text{C}_2\text{H}_5)_2\text{O}$ molecules, obtained from B3LYP/6-31+G(d,p) calculations

Parameter ^a	<i>trans</i> -HONO			<i>cis</i> -HONO		
	Monomer	$(\text{CH}_3)_2\text{O} \cdots \text{HONO}$	$(\text{C}_2\text{H}_5)_2\text{O} \cdots \text{HONO}$	Monomer	$(\text{CH}_3)_2\text{O} \cdots \text{HONO}$	$(\text{C}_2\text{H}_5)_2\text{O} \cdots \text{HONO}$
Bond length^b						
R(O ₁ N ₂)	1.179	1.188	1.189	1.190	1.200	1.200
R(N ₂ O ₃)	1.427	1.388	1.387	1.387	1.364	1.364
R(O ₃ H ₄)	0.972	0.993	0.995	0.984	1.004	1.009
R(H ₄ · · · O ₅)	—	1.733	1.723	—	1.731	1.719
R(O ₅ C ₆)	1.415, 1.424 ^c	1.423	1.436	1.415	1.423	1.439
R(O ₅ C ₇)	1.415, 1.423 ^c	1.425	1.435	1.415	1.425	1.438
R(C ₆ C ₈)	1.529	—	1.525	1.529	—	1.525
R(C ₇ C ₁₁)	1.520	—	1.519	1.520	—	1.519
Angle^d						
O ₃ N ₂ O ₁	110.9	111.9	—	113.52	114.2	114.2
H ₄ O ₃ N ₂	103.1	103.7	—	106.64	109.3	109.5
C ₆ O ₅ · · · H ₄	—	124.4	—	—	123.7	110.5
C ₇ O ₅ · · · H ₄	—	121.7	—	—	122.3	115.8
C ₇ O ₅ C ₆	112.7, 115.0 ^e	113.9	—	112.7; 115.0 ^c	114.0	114.7
C ₈ C ₆ O ₅	113.93	—	—	113.9	—	112.8
C ₁₁ C ₇ O ₅	108.38	—	—	108.4	—	108.9
E_{tot} (a.u.)	−205.715014 ^e	−360.770482	−439.413921	−205.714283 ^f	−360.769263	−439.411813
	−155.041313 ^g	—	—	−155.041313 ^g	—	—
	−233.684375 ^h	—	—	−233.684375 ^h	—	—

^a See Figs. 1 and 2 for numbering of atoms.^b In angstrom.^c Parameters for $(\text{C}_2\text{H}_5)_2\text{O}$.^d In degrees.^e E^{tot} for *trans*-HONO.^f E^{tot} for *cis*-HONO.^g E^{tot} for $(\text{CH}_3)_2\text{O}$.^h E^{tot} for $(\text{C}_2\text{H}_5)_2\text{O}$.

with the 6-311++G(d,p) basis set and B3LYP calculations (see Tables 3–5).

The calculated vibrational frequencies and infrared intensities are presented in Table 3 together with the available experimental data. In Table 3 is included a detailed description of the normal modes of the monomers based on the potential energy distribution (PED) obtained from MP2/6-311++G(d,p) calculations.

The aim is to establish the accuracy of the calculations used in the study and to define the ‘optimal’ scale factors for each vibration from the ratio $v_i^{\text{exp}} / v_i^{\text{calc}}$. The concept of the ‘optimal’ scale factor has been proposed by Destexhe et al. [20] in order to obtain an estimation of the anharmonicity of the modes in H-bonded H_2O with pyridine. This procedure could only be applied for modes, which are experimentally accessible in the spectral region. In the present study the ‘optimal’ scale factors for the stretching and bending vibrations of the monomers are shown in Table 3.

The results in Table 3 show that the calculated vibrational frequencies at the MP2 level are in better agreement with the experimental data, than the frequencies calculated at the SCF level. The predicted values with B3LYP calculations are very near to the results, obtained with MP2/6-311++G(d,p).

The next step in the study is to predict the vibrational frequencies and infrared intensities for the hydrogen-bonded complexes $(\text{CH}_3)_2\text{O} \cdots \text{HONO}-\text{trans}$ (**1A**) and $(\text{CH}_3)_2\text{O} \cdots \text{HONO}-\text{cis}$ (**1B**) and to estimate the changes in the vibrational characteristics arising from the hydrogen bonding. The predicted vibrational characteristics and PED’s elements for the complexes **1A** and **1B** are shown in Tables 4 and 5. The potential energy distribution (PED), obtained from MP2/6-311++G(d,p) calculations is used for a

Table 2

Dissociation energies (uncorrected and corrected), basis set superposition error (BSSE) and zero-point energy differences ΔE (zp vib) in kcal mol^{−1} calculated with B3LYP/6-31+G(d,p) calculations for the complexes, shown in Figs. 1 and 2

Complex	ΔE (ucorr)	BSSE	ΔE (zp vib)	^a Total correction	ΔE (corr)	$R(\text{H}_4 \cdots \text{O}_5)$ (Å)
1A (trans)	−8.88	0.88	1.23	2.11	−6.77	1.733
1B (cis)	−8.57	0.94	1.21	2.15	−6.42	1.731
2A (trans)	−9.12	1.01	1.40	2.41	−6.71	1.723
2B (cis)	−8.25	0.62	1.24	1.86	−6.39	1.719

Table 3

Experimental and calculated vibrational characteristics (ν in cm^{-1} , A in km mol^{-1}) for *trans*-HONO, *cis*-HONO and $(\text{CH}_3)_2\text{O}$

Mode	Approximate description (PED) ^a	Experimental ^b		SCF/6-311++G ^{**}		MP2/6-311++G ^{**}		B3LYP/6-31+G(d,p)		B3LYP/6-31G(d,p)	
		ν	A	$\nu/\text{scale factor}$	A	$\nu/\text{scale factor}$	A	$\nu/\text{scale factor}$	A	$\nu/\text{scale factor}$	A
<i>trans</i> -HONO											
ν_1	100 $\nu(\text{O}-\text{H})$	3572.63568.5		4134/0.86420.8632	145.2	3811/0.93740.9364	94.0	3749/0.95300.9519	80.9	3756/0.95120.9501	57.3
ν_2	89 $\nu(\text{N}=\text{O})$	1689.11688.0	s	2025/0.83410.8334	188.3	1672/1.01021.0096	107.8	1783/0.94730.9467	178.7	1792/0.94260.9420	135.4
ν_3	85 $\delta(\text{NOH}) + 11 \nu(\text{N}=\text{O})$	1265.81263.9		1492/0.84840.8471	260.9	1294/0.97820.9767	189.6	1297/0.97600.9738	188.4	1308/0.96770.9663	187.5
ν_4	49 $\delta(\text{NOH}) + 42 \nu(\text{N}=\text{O})^c$	800.4796.6	s	1081/0.74040.7369	255.0	826/0.96900.9644	177.7	831/0.96320.9586	159.0	862/0.92850.9241	144.2
ν_5	60 $\nu(\text{N}=\text{O}) + 40 \delta(\text{ONO})^d$	608.7		794/0.7666	24.5	616/0.9882	176.7	628/0.9693	118.4	631/0.9647	83.0
ν_6	100 $\tau(\text{HONO})$	549.4548.2	s	582/0.94400.9419	139.2	565/0.97240.9703	116.4	586/0.93750.9355	118.1	595/0.92340.9214	105.8
<i>cis</i> -HONO											
ν_1	100 $\nu(\text{O}-\text{H})$	3412.43410.7		3961/0.86150.8610	71.1	3552/0.96070.9602	37.5	3575/0.95450.9540	26.3	3575/0.95450.9540	15.2
ν_2	77 $\nu(\text{N}=\text{O}) + 17 \delta(\text{NOH})$	1634.01632.8	s	1969/0.82990.8292	264.3	1545/1.05761.0568	126.4	1714/0.95330.9526	216.0	1726/0.94670.9460	171.5
ν_3	71 $\delta(\text{NOH}) + 23 \nu(\text{N}=\text{O})$	—		1509	9.4	1306	7.1	1332	6.5	1349	5.8
ν_4	41 $\delta(\text{ONO}) + 47 \nu(\text{N}=\text{O})^e$	853.1850.2		1144/0.74570.7432	379.9	898/0.950.9468	376.3	897/0.95110.9478	325.6	922/0.92530.9221	264.8
ν_5	100 $\tau(\text{HONO})^f$	—		782	14.7	706	121.9	698	119.0	736	108.9
ν_6	53 $\nu(\text{N}=\text{O}) + 46 \delta(\text{ONO})^g$	638.4		706/0.9042	152.6	624/1.0231	46.8	639/0.9991	22.9	648/0.9852	14.9
$(\text{CH}_3)_2\text{O}$											
ν_7	93 $\nu(\text{C}_3-\text{H}_6)$	2986		3270/0.913	42.2	3194/0.935	23.5	3132/0.953	22.4	3127/0.955	29.4
ν_8	91 $\nu(\text{C}_1-\text{H}_8)$	2986		3254/0.918	45.5	3177/0.940	24.3	3131/0.954	32.8	3126/0.955	35.2
ν_9	98 $\nu(\text{CH}_3)^{\text{as}}$	2922		3170/0.922	160.5	3087/0.946	1.2	3027/0.965	0.0	3019/0.968	0.0
ν_{10}	100 $\nu(\text{CH}_3)^{\text{as}}$	2922		3168/0.922	2.7	3081/0.948	118.4	3022/0.967	147.4	3015/0.969	155.5
ν_{11}	94 $\nu(\text{CH}_3)^{\text{sym}}$	2889		3130/0.923	85.0	3022/0.956	68.1	2984/0.968	73.6	2981/0.968	61.4
ν_{12}	100 $\nu(\text{CH}_3)^{\text{as}}$	2820		3116/0.905	53.9	3014/0.936	51.6	2971/0.949	65.9	2966/0.951	58.2
ν_{13}	56 $\tau(\text{HCOC}) + 44 \delta(\text{HCO})$	—		1638	1.5	1545	1.6	1517	2.3	1535	0.4
ν_{14}	81 $\tau(\text{HCOC})$	—		1620	12.8	1525	12.7	1499	14.7	1511	13.4
ν_{15}	84 $\tau(\text{HCOC})$	—		1619	12.9	1511	13.5	1495	14.3	1504	0.1
ν_{16}	78 $\delta(\text{HCO})$	—		1617	2.0	1506	0.3	1489	0.5	1503	9.2
ν_{17}	84 $\tau(\text{HCOC})$	—		1608	0.0	1500	0.0	1485	0.0	1493	0.0
ν_{18}	100 $\delta(\text{HCO})$	—		1583	7.4	1480	3.3	1463	3.9	1472	10.4
ν_{19}	69 $\delta(\text{HCO}) + 10 \delta(\text{COC})$	1168		1385/0.843	11.9	1282/0.911	6.2	1264/0.924	5.2	1273/0.918	4.8
ν_{20}	68 $\nu(\text{C}-\text{O})^{\text{as}}$	1098		1334/0.823	165.9	1222/0.898	109.0	1199/0.915	104.1	1210/0.907	110.7
ν_{21}	83 $\delta(\text{HCO})$	—		1300	12.1	1212	8.0	1192	8.0	1203	6.2
ν_{22}	84 $\delta(\text{HCO})$	—		1265	0.0	1176	0.0	1161	0.0	1168	0.0
ν_{23}	35 $\nu(\text{C}-\text{O})^{\text{as}} + 40 \delta(\text{HCO})$	1098		1214/0.904	37.8	1135/0.967	26.7	1119/0.981	43.3	1131/0.970	34.1
ν_{24}	97 $\nu(\text{C}-\text{O})^{\text{sym}}$	925		1033/0.895	45.2	968/0.955	40.0	939/0.985	41.0	955/0.968	34.3
ν_{25}	91 $\delta(\text{COC})$	—		435	2.6	419	1.8	410	2.6	414	2.7
ν_{26}	94 $\tau(\text{HCOC})$	—		266	7.2	267	6.0	243	7.3	249	6.2
ν_{27}	100 $\tau(\text{HCOC})$	—		220	0.0	215	0.0	212	0.0	223	0.0

^a PEDs elements lower than 10% are not included. PEDs elements obtained with MP2/6-311++G(d,p) are given.^b Ref. [14] for HONO; [26] for $(\text{CH}_3)_2\text{O}$. PEDs with SCF/6-311++G(d,p) for *trans*-HONO:^c 86 $\nu(\text{N}=\text{O})$.^d 80 $\delta(\text{ONO})$. PEDs with SCF/6-311++G(d,p) for *cis*-HONO.^e 82 $\nu(\text{N}=\text{O})$.^f 73 $\delta(\text{ONO}) + 20 \nu(\text{N}=\text{O})$.^g 100 $\tau(\text{HONO})$.

Table 4

Calculated vibrational characteristics (ν in cm^{-1} , A in km mol^{-1}) for the hydrogen-bonded complex $(\text{CH}_3)_2\text{O} \cdots \text{HONO-trans}$

Mode	Approximate description (PED) ^a	SCF/6-311++G**		MP2/6-311++G**		B3LYP/6-31+G(d,p)		B3LYP/6-31G(d,p)	
		$\nu/\Delta\nu^{\text{scal}}$	$A/\Delta A$	$\nu/\Delta\nu^{\text{scal}}$	$A/\Delta A$	$\nu/\Delta\nu^{\text{scal}}$	$A/\Delta A$	$\nu/\Delta\nu^{\text{scal}}$	$A/\Delta A$
ν_1	100 $\nu(\text{O-H})$	3939/-169	913.9/768.7	3507/-285	1179.5/1085.5	3366/-365	1243.5/1162.1	3429/-311	1025.4/968.1
ν_2	98 $\nu(\text{C-H})$	3267/-3	27.9/-14.3	3186/-7	9.1/-14.4	3151/18	8.8/-13.6	3155/27	6.4/-23
ν_3	93 $\nu(\text{C-H})$	3255/1	31.3/-14.2	3177/0	15.0/-9.3	3146/14	14.5/-18.3	3144/17	17.9/-17.3
ν_4	100 $\nu(\text{C-H})$	3211/38	109.1/-155.6	3127/38	0.9/-0.3	3071/42	0.4/0.4	3065/45	6.2/6.2
ν_5	98 $\nu(\text{C-H})$	3209/38	4.9/106.4	3122/39	74.8/-43.6	3067/44	89.3/-58.1	3061/45	96.8/-58.7
ν_6	90 $\nu(\text{C-H})$	3155/23	70.7/-14.3	3046/23	71.2/3.1	3012/27	92.1/18.5	3010/28	79.0/17.6
ν_7	95 $\nu(\text{C-H})$	3144/25	49.8/-4.1	3041/25	41.5/-10.1	3005/32	48.2/-17.7	3001/33	42.3/-15.9
ν_8	65 $\nu(\text{N=O}) + 25 \delta(\text{HON})$	2002/-19	210.9/22.6	1653/-19	59.0/51.2	1775/-8	166.4/7.7	1761/-29	143.3/7.9
ν_9	60 $\tau(\text{HCOC}) + 30 \delta(\text{HCO})$	1634/-4	11.1/9.6	1542/-3	1.7/0.1	1518/1	3.4/1.1	1533/-2	0.3/-0.1
ν_{10}	80 $\tau(\text{HCOC})$	1622/2	2.8/-10	1525/0	11.3/-1.4	1500/1	9.9/-4.8	1512/1	10.3/-3.1
ν_{11}	85 $\delta(\text{HCO})$	1621/4	50.4/48.4	1510/4	0.7/0.4	1497/8	17.3/16.8	1508/5	11.9/2.7
ν_{12}	83 $\tau(\text{HCOC})^b$	1620/109	17.0/-243.9	1509/-2	17.2/3.7	1491/-4	3.5/-10.8	1505/1	0.4/0.3
ν_{13}	81 $\tau(\text{HCOC})$	1613/5	214.1/214.1	1499/-1	0.7/0.7	1487/2	0.5/0.5	1496/3	1.2/1.2
ν_{14}	100 $\delta(\text{HCO})$	1608/25	0.1/-7.3	1485/5	34.8/31.5	1479/16	160.8/49.6	1486/14	118.5/40.3
ν_{15}	43 $\delta(\text{HON}) + 29 \nu(\text{N=O})^c$	1583/0	14.1/6.7	1459/161	187.4/7.8	1459/158	53.5/-27.6	1466/153	50.7/-69
ν_{16}	58 $\delta(\text{HCO})$	1394/8	16.0/4.1	1292/9	8.4/2.2	1276/11	6.8/1.6	1285/11	4.0/-0.8
ν_{17}	55 $\nu(\text{C-O}) + 20 \delta(\text{HCO})$	1318/-13	126.7/-39.2	1214/-7	75.6/-33.4	1192/-6	4.7/-99.4	1203/-6	4.0/-106.7
ν_{18}	82 $\delta(\text{HCO})$	1297/-3	11.1/-1	1206/-6	6.0/-2	1189/-3	66.5/58.5	1202/-1	73.5/67.3
ν_{19}	84 $\delta(\text{HCO})$	1260/-5	0.0/0.0	1169/-7	0.0/0.0	1162/1	0.0/0.0	1170/2	0.0/0.0
ν_{20}	77 $\delta(\text{HCO})$	1212/-2	65.2/27.4	1135/0	44.9/18.2	1114/-5	62.8/19.5	1127/-4	56.1/22.0
ν_{21}	73 $\nu(\text{C-O}) + 17 \nu(\text{O-N})^d$	1149/50	275.1/20.1	965/-3	53.9/13.9	937/-2	44.6/3.6	955/0.0	67.3/33.0
ν_{22}	51 $\nu(\text{O-N}) + 23 \delta(\text{ONO})$	1017/171	106.0/81.5	927/307	343.7/167	904/267	311.7/193.3	928/286	230.7/147.7
ν_{23}	55 $\tau(\text{HONO})$	842/296	120.0/-19.2	792/221	86.0/-30.4	864/261	87.8/-30.3	808/197	79.3/-26.5
ν_{24}	63 $\delta(\text{ONO}) + 33 \nu(\text{O-N})$	833/30	3.5/-21	715/98	43.6/-133.1	706/76	35.1/-83.3	703/69	22.0/-61
ν_{25}	82 $\delta(\text{CO} \cdots \text{H})$	447	8.9	427	11.5	418	14.0	425	13.0
ν_{26}	87 $\tau(\text{HCOC})$	247/-19	7.7/0.5	230/-37	5.0/-1	231/-12	5.8/-1.5	251/2	4.3/1.9
ν_{27}	62 $\nu(\text{O} \cdots \text{H}) + 33 \delta(\text{CO} \cdots \text{H})$	174	5.5	187	9.9	195	0.0	213	0.7
ν_{28}	84 $\tau(\text{HCOC})$	167/-53	0.0/0.0	161/-54	0.0/0.0	185/-27	10.3/10.3	192/-31	10.1/10.1
ν_{29}	45 $\delta(\text{CO} \cdots \text{H}) + 30 \nu(\text{O} \cdots \text{H})$	136	7.9	123	1.2	139	4.7	140	5.1
ν_{30}	44 $\tau(\text{HCOC})$	117/-103	1.2/1.2	115/-100	3.9/3.9	123/-89	1.9/1.9	126/-97	1.1/1.1
ν_{31}	100 $\tau(\text{CO} \cdots \text{HO})$	59	3.6	112	7.5	39	0.4	66	1.8
ν_{32}	60 $\delta(\text{O} \cdots \text{HO})$	42	0.4	49	0.5	43	0.5	45	0.4
ν_{33}	48 $\tau(\text{CO} \cdots \text{HO})$	22	0.2	25	0.0	20	0.2	39	0.2

^a PEDs elements lower than 10% are not included. PEDs elements obtained with MP2/6-311++G** are given. PEDs with SCF/6-311++G(d,p):^b 40 $\delta(\text{HON})$.^c 76 $\delta(\text{HCO})$.^d 88 $\nu(\text{N-O})$.

Table 5

Calculated vibrational characteristics (ν in cm^{-1} , A in km mol^{-1}) for the hydrogen-bonded complex $(\text{CH}_3)_2\text{O} \cdots \text{HONO}-\text{cis}$

Mode	Approximate description (PED) ^a	SCF/6-311++G ^{**}		MP2/6-311++G ^{**}		B3LYP/6-31+G(d,p)		B3LYP/6-31G(d,p)	
		$\nu/\Delta\nu^{\text{scal}}$	$A/\Delta A$						
ν_1	100 $\nu(\text{O}-\text{H})$	3794/−144	652.3/581.2	3339/−205	869.9/832.4	3191/−367	916.3/890.0	3233/−326	799.4/784.2
ν_2	95 $\nu(\text{C}-\text{H})$	3281/10	30.1/−12.1	3204/9	12.9/−10.6	3159/26	6.1/−16.3	3164/35	4.7/−24.7
ν_3	100 $\nu(\text{C}-\text{H})$	3271/16	20.3/−25.2	3189/11	8.2/−16.1	3144/12	11.7/−21.1	3143/16	15.3/−19.9
ν_4	98 $\nu(\text{C}-\text{H})$	3208/35	101.6/−58.9	3127/38	0.7/−0.5	3070/41	0.5/0.5	3064/44	3.8/3.8
ν_5	100 $\nu(\text{C}-\text{H})$	3206/35	18.6/15.9	3122/39	77.6/−40.8	3066/43	91.2/−56.2	3061/45	101.5/−54
ν_6	98 $\nu(\text{C}-\text{H})$	3155/23	79.0/−6.0	3048/25	79.1/11.0	3012/27	117.2/43.6	3010/28	95.5/34.1
ν_7	98 $\nu(\text{C}-\text{H})$	3143/24	45.9/−8.0	3043/27	41.2/−10.4	3004/31	48.5/−17.4	3001/33	42.4/−15.8
ν_8	65 $\nu(\text{N}=\text{O}) + 24 \delta(\text{HON})$	1941/−23	251.3/−13.0	1606/65	150.4/24.4	1674/−38	203.9/−12.1	1687/−37	162.6/−8.9
ν_9	60 $\tau(\text{HCOC}) + 31 \delta(\text{HCO})$	1634/−4	3.5/2.0	1542/−3	2.0/0.4	1518/1	2.9/0.6	1532/−3	0.7/0.3
ν_{10}	79 $\tau(\text{HCOC})$	1622/2	2.6/−10.2	1525/0	16.0/3.3	1501/2	15.7/1.0	1511/0.0	16.6/3.2
ν_{11}	82 $\tau(\text{HCOC})$	1622/3	15.0/2.1	1512/1	16.1/2.6	1500/5	17.5/3.2	1510/6	11.2/11.1
ν_{12}	70 $\delta(\text{HCO})$	1618/1	14.2/12.2	1509/3	3.4/3.1	1489/0.0	2.4/1.9	1501/−2	2.5/−6.7
ν_{13}	78 $\tau(\text{HCOC})$	1609/1	0.6/0.6	1501/1	1.6/1.6	1488/3	1.7/1.7	1496/3	2.0/2.0
ν_{14}	76 $\delta(\text{HCO})$	1602/21	31.5/24.1	1484/4	0.7/−2.6	1466/3	8.1/4.2	1474/2	10.8/0.4
ν_{15}	47 $\delta(\text{HON}) + 32 \nu(\text{N}=\text{O})$	1584/75	5.2/−4.2	1443/137	30.9/23.8	1449/117	31.7/25.2	1457/108	21.5/15.7
ν_{16}	56 $\delta(\text{HCO})$	1395/8	14.7/2.8	1293/10	7.3/1.1	1276/11	5.2/0.0	1283/9	2.7/−2.1
ν_{17}	54 $\nu(\text{C}-\text{O}) + 21 \delta(\text{HCO})$	1320/96	57.2/19.4	1215/77	94.0/67.3	1193/73	4.3/−39.0	1203/70	3.7/−30.4
ν_{18}	82 $\delta(\text{HCO})$	1298/−2	11.0/−1.1	1208/−4	5.6/−2.4	1190/−2	81.8/73.8	1202/−1	91.6/85.4
ν_{19}	83 $\delta(\text{HCO})$	1262/−3	0.0/0.0	1171/−5	0.0/0.0	1163/−2	0.0/0.0	1170/2	0.0/0.0
ν_{20}	46 $\nu(\text{C}-\text{O}) + 32 \delta(\text{HCO})$	1215/1	162.9/125.1	1137/2	50.7/24	1114/−5	72.0/28.7	1125/−6	60.6/26.5
ν_{21}	64 $\nu(\text{N}-\text{O}) + 26 \delta(\text{ONO})$	1201/42	133.4/−46.5	1015/400	301.8/255.0	988/349	249.2/226.3	1012/359	206.5/191.6
ν_{22}	95 $\nu(\text{C}-\text{O})$	1017/−14	84.6/39.4	951/−16	119.6/79.6	923/−16	113.9/72.9	940/−15	92.9/58.6
ν_{23}	63 $\tau(\text{HONO}) + 37 \tau(\text{O} \cdots \text{HON})$	900/175	136.9/−15.7	847/141	96.8/−25.1	919/221	94.8/−24.2	901/165	90.6/−18.3
ν_{24}	61 $\delta(\text{ONO}) + 33 \nu(\text{N}-\text{O})$	820/38	11.5/−3.2	708/86	20.6/−26.2	697/58	18.7/−4.2	704/55	12.3/−2.6
ν_{25}	83 $\delta(\text{CO} \cdots \text{H})$	451	8.5	432	9.7	420	12.9	425	12.9
ν_{26}	89 $\tau(\text{HCOC})$	255/−11	7.9/0.7	240/−27	4.5/−1.5	237/−6	5.5/−1.8	246/−3	3.8/−2.4
ν_{27}	59 $\nu(\text{O} \cdots \text{H}) + 28 \delta(\text{CO} \cdots \text{H})$	182/	2.6	191	8.6	202	0.8	214	1.4
ν_{28}	70 $\tau(\text{HCOC})$	180/−40	5.2/5.2	172/−43	0.0/0.0	188/−24	10.4/10.4	191/−32	9.1/9.1
ν_{29}	47 $\delta(\text{CO} \cdots \text{H}) + 32 \nu(\text{O} \cdots \text{H})$	176	0.5	137	5.6	182	3.2	178	4.4
ν_{30}	58 $\tau(\text{HCOC})$	116/−104	0.9/0.9	123/−92	1.1/1.1	112/−100	1.2/1.2	121/−102	0.5/0.5
ν_{31}	100 $\tau(\text{CO} \cdots \text{HO})$	73	0.4	98	7.5	77	0.5	100	1.5
ν_{32}	61 $\delta(\text{O} \cdots \text{HO})$	53	0.1	89	0.3	29	0.0	44	0.0
ν_{33}	87 $\tau(\text{O} \cdots \text{HON})$	34	0.3	26	0.2	26	3.9	33	3.8

^a PEDs elements lower than 10% are not included. PEDs elements obtained with MP2/6-311++G^{**} are given.

description of the normal modes. The results for PED show that most of the intramolecular vibrations of the dimers can be correlated with normal modes of the monomers, described in Table 3. The hydrogen bonding leads to the changes in the percentage contributions (PED's elements) of localised modes to each normal mode in the monomers. There are six more intermolecular vibrations (see Tables 4 and 5), which arise from the complexation: the stretching C · · · H vibration, the torsional vibrations and in plane bending vibrations.

The predicted values of the stretching O · · · H vibration for the complex $(\text{CH}_3)_2\text{O} \cdots \text{HONO-}trans$ (see Table 4) are at: 174–213 cm^{-1} , with weak infrared intensity. The deformation intermolecular vibrations (ν_{29} , ν_{31} , ν_{32} , and ν_{33}) are predicted are at: 20–140 cm^{-1} , while the vibration $\delta(\text{CO} \cdots \text{H})$ (ν_{29}) is calculated in the range: 418–447 cm^{-1} .

For the complex $(\text{CH}_3)_2\text{O} \cdots \text{HONO-}cis$ the predicted values of the stretching C · · · H vibration (see Table 5) are in the range: 182–214 cm^{-1} . The torsional (ν_{31} and ν_{33}) and in plane bending vibration $\delta(\text{O} \cdots \text{HO})$ (ν_{32}), are predicted in the range: 26–100 cm^{-1} , while the vibration $\delta(\text{CO} \cdots \text{H})$ (ν_{25}) is calculated in the range: 420–451 cm^{-1} .

The changes in the vibrational characteristics (vibrational frequencies and infrared intensities) from free monomers to complexes arising from the hydrogen bonding have been estimated. The shifts in the vibrational characteristics ($\Delta\nu^{\text{scal}}$) of HONO (*trans*, *cis*) and $(\text{CH}_3)_2\text{O}$ upon formation of the hydrogen-bonded complexes have been calculated by ab initio and B3LYP calculations. The corresponding scale factor is used for each vibration. The predicted frequency shift is

$$\Delta\nu_i^{\text{scal}} = k_i(\nu_i^{\text{complex}} - \nu_i^{\text{monomer}})$$

where k_i is the corresponding ‘optimal’ scale factor.

In our previous studies [21–25] it was established that the hydrogen bonding leads to the substantial changes in the vibrational characteristics for the vibrations of the monomer bonds participating in the hydrogen bonding. As can be seen from the results, presented in Tables 4 and 5, these vibrations are: the stretching O–H and O–N vibrations and the deformation $\delta(\text{ONO})$, $\delta(\text{HON})$ and torsional HONO vibrations. The most sensitive to the complexation is the stretching O–H vibration (ν_1). Its vibrational frequency in the complexes is shifted to lower wavenumbers. The calculated frequency shift $\Delta\nu(\text{O–H})$ for the complex $(\text{CH}_3)_2\text{O} \cdots \text{HONO-}trans$ (**1A**) is larger than for the complex $(\text{CH}_3)_2\text{O} \cdots \text{HONO-}trans$ (**1B**). In the same time the intensity of this vibration increases dramatically upon hydrogen bonding. The calculated increase for the complex **1A** is 18 times and for the complex **1B** is 53 times.

The results from the calculations show that the torsional HONO vibration is very sensitive to the complexation. Its vibrational frequency in the complexes **1A** and **1B** (ν_{23}) is shifted to higher frequencies. The predicted changes in the vibrational frequency for the complex $(\text{CH}_3)_2\text{O} \cdots \text{HONO-}trans$ (**1A**) are larger than for the complex $(\text{CH}_3)_2\text{O} \cdots \text{HONO-}cis$ (**1B**). The ab initio and DFT

Table 6
Calculated and experimentally observed changes in the vibrational characteristics (ν in cm^{-1} , A in km mol^{-1}) for *trans*-HONO hydrogen-bonded with $(\text{CH}_3)_2\text{O}$ (DME) and $(\text{C}_2\text{H}_5)_2\text{O}$ (DEE)

Mode	Experimental [16]	$\Delta\nu$	MP2/6-31+G(d,p)			B3LYP/6-31G(d,p)			DME			DEE		
			DME		DEE	DME		DEE	DME		DEE	DME		DEE
			$\Delta\nu^{\text{scal}}$	ΔA	$\Delta\nu^{\text{scal}}$	ΔA	$\Delta\nu^{\text{scal}}$	ΔA	$\Delta\nu^{\text{scal}}$	ΔA	$\Delta\nu^{\text{scal}}$	ΔA	$\Delta\nu^{\text{scal}}$	ΔA
<i>trans</i> -HONO														
$\nu(\text{O–H})$	-376		-298	1086.0	-497	1341.4	-364	1162.6	-410	1232.9	-311	968.1	-380	1103.0
$\nu(\text{N=O})$	-		-14	-47.8	-24	-40.6	-8	7.7	-43	0.2	-29	7.9	-32	8.3
$\delta(\text{NOH})$	112		161	-12.4	156	-24.1	158	-27.6	142	-87.2	153	-69.0	151	-22.5
$\nu(\text{N–O})$	44		103	161.3	120	115.3	267	193.3	275	133.5	286	147.7	269	149.7
$\delta(\text{ONO})$	-		101	-130.1	103	-139.3	75	-83.3	76	-84.6	69	-61.0	71	-61.5
$\tau(\text{HONO})$	31		277	-30.8	267	-57.1	260	-30.3	237	-17.6	196	-26.5	185	-19.1

calculations predicted a decrease of the infrared intensity for the torsional HONO vibration in the complexes.

The calculations used in this study show that the modes ν_{22} and ν_{24} for the complex **1A** and ν_{21} and ν_{24} for the complex **1B** are mixed modes including a deformation ONO and a stretching O–N vibrations. These vibrations are also sensitive to the complexation. Their vibrational frequencies in the complexes are shifted to higher wave numbers. The intensities of the vibrations ν_{22} (**1A**) and ν_{21} (**1B**) increase in the complexes, while the intensities of the vibrations ν_{24} (**1A**, **1B**) decrease upon hydrogen bond formation.

The vibrational characteristics (vibrational frequency and infrared intensity) of the deformation $\delta(\text{HON})$ vibration ν_{15} (**1A**, **1B**) are changed also in the complexes. As can be seen from the results presented in Tables 4 and 5, the ab initio and B3LYP calculated vibrational frequencies for the complexes **1A** and **1B** (ν_{15}) are shifted to higher frequencies. The predicted changes in the vibrational frequency for the complex $(\text{CH}_3)_2\text{O} \cdots \text{HONO}-\text{trans}$ (**1A**) are larger than for the complex $(\text{CH}_3)_2\text{O} \cdots \text{HONO}-\text{cis}$ (**1B**). The infrared intensity of the deformation $\delta(\text{HON})$ vibration changes negligibly upon complexation.

It is seen that the stretching C–H vibrations (from $(\text{CH}_3)_2\text{O}$) are less sensitive to the formation of hydrogen bonds. In the complexes **1A** and **1B** their vibrational frequencies are shifted to higher wave numbers. In more cases the infrared intensities of these vibrations decrease.

The infrared matrix isolation study of the hydrogen-bonded complex formed between *trans*-HONO and diethyl ether [16] provide very common information about the hydrogen bonding and structure of this system. The observed shifts in the vibrational frequencies of the $\nu(\text{O–H})$ (-376 cm^{-1}) and $\delta(\text{NOH})$ (112 cm^{-1}) are indicative of strong intermolecular hydrogen bonds.

Bearing in mind that the stability of the complexes of dimethyl and diethyl ethers with *trans*-HONO are very near (see Table 2), the calculated changes in the vibrational frequencies for these complexes are compared with the experimentally observed for the complex formed between *trans*-HONO and diethyl ether. As can be seen from the results presented in Table 6, the calculated shifts in the vibrational frequencies for the complexes of dimethyl and diethyl ethers with *trans*-HONO are very near and in agreement with the experimentally observed [16].

3. Conclusions

The ab initio and DFT calculations show that the changes in the vibrational characteristics (vibrational frequencies and infrared intensities) upon hydrogen bonding for the hydrogen-bonded complex $(\text{CH}_3)_2\text{O} \cdots \text{HONO}-\text{trans}$ are larger than for the complex $(\text{CH}_3)_2\text{O} \cdots \text{HONO}-\text{cis}$.

The most sensitive to the complexation is the stretching O–H vibration (ν_1). Its vibrational frequency in

the complexes is shifted to lower wavenumbers. The calculated frequency shift $\Delta\nu(\text{O–H})$ for the complex $(\text{CH}_3)_2\text{O} \cdots \text{HONO}-\text{trans}$ (**1A**) is larger than for the complex $(\text{CH}_3)_2\text{O} \cdots \text{HONO}-\text{trans}$ (**1B**). In the same time the intensity of this vibration increases dramatically upon hydrogen bonding. The calculated increase for the complex **1A** is 18 times and for the complex **1B** is 53 times.

References

- [1] J. Sadlej, V. Buch, J. Chem. Phys. 100 (1994) 4272.
- [2] J. Sadlej, B. Rowland, J.P. Devlin, V. Buch, J. Chem. Phys. 102 (1995) 4804.
- [3] Z. Mielke, Z. Latajka, J. Kolodziej, K.G. Toknadze, J. Phys. Chem. 100 (1996) 11610.
- [4] B.J. Gertner, J.T. Hynes, Science 271 (1996) 1563.
- [5] A.J. Barnes, E. Lasson, C.J. Nielsen, J. Chem. Soc., Faraday Trans. 91 (1995) 3111.
- [6] M.-T. Nguyen, A.J. Jamka, R.A. Cazar, F.-M. Tao, J. Chem. Phys. 106 (1997) 8710.
- [7] J. Lundell, Z. Latajka, J. Phys. Chem. A 101 (1997) 5004.
- [8] J.P.D. Abbath, G.C.H. Washewsky, J. Phys. Chem. A 102 (1998) 3719.
- [9] F.-M. Tao, J. Chem. Phys. 108 (1998) 193.
- [10] R.N. Musin, M.C. Lin, J. Phys. Chem. A 102 (1998) 1808.
- [11] J.V. Bevan, in: A. Weber (Ed.), Structure and Dynamics of Weakly Bound Molecular Complexes, Reidel, Dordrecht, 1987, p. 149.
- [12] L. Andrews, in: L. Andrews, M. Moskovits (Eds.), Chemical and Physics of Matrix Isolated Species, North Holland/Oxford, Amsterdam/New York, 1989, p. 15.
- [13] Z. Mielke, Z. Latajka, J. Kolodziej, K.G. Tokhadze, J. Phys. Chem. 100 (1996) 11610.
- [14] Z. Mielke, K.G. Tokhadze, Z. Latajka, E. Ratajczak, J. Phys. Chem. 100 (1996) 539.
- [15] M. Krajewska, Z. Mielke, K.G. Tokhadze, J. Mol. Struct. 404 (1997) 47.
- [16] Z. Mielke, M. Wierzejewska, A. Olbert, M. Krajewska, K.G. Tokhadze, J. Mol. Struct. 436–437 (1997) 339.
- [17] B.J. Finlayson-Pitts, J.N. Pitts Jr., Atmospheric Chemistry: Fundamentals and Experimental Techniques, Wiley, New York, 1986.
- [18] A.J. Barnes, M.P. Wright, J. Mol. Struct. (Theochem.) 135 (1985) 21.
- [19] M.J. Frisch, G.W. Trucks, H.B. Schlegel, G.E. Scuseria, M.A. Robb, J.R. Cheeseman, V.G. Zakrzewski, J.A. Montgomery Jr., R.E. Stratmann, J.C. Burant, S. Dapprich, J.M. Millam, A.D. Daniels, K.N. Kudin, M.C. Strain, O. Farkas, J. Tomasi, V. Barone, M. Cossi, R. Cammi, B. Mennucci, C. Pomelli, C. Adamo, S. Clifford, J. Ochterski, G.A. Petersson, P.Y. Ayala, Q. Cui, K. Morokuma, D.K. Malick, A.D. Rabuck, K. Raghavachari, J.B. Foresman, J. Cioslowski, J.V. Ortiz, A.G. Baboul, B.B. Stefanov, G. Liu, A. Liashenko, P. Piskorz, I. Komaromi, R. Gomperts, R.L. Martin, D.J. Fox, T. Keith, M.A. Al-Laham, C.Y. Peng, A. Nanayakkara, C. Gonzalez, M. Challacombe, P.M.W. Gill, B. Johnson, W. Chen, M.W. Wong, J.L. Andres, C. Gonzalez, M. Head-Gordon, E.S. Replogle, J.A. Pople, Gaussian 98, Revision A.7, Gaussian, Inc., Pittsburgh, PA, 1998.
- [20] A. Destexhe, J. Smets, L. Adamowicz, G. Maes, J. Phys. Chem. 98 (1994) 1506.
- [21] Y. Dimitrova, S.D. Peyerimhoff, Chem. Phys. 254 (2000) 125.
- [22] Y. Dimitrova, J. Mol. Struct. (Theochem.) 532 (2000) 41.
- [23] Y. Dimitrova, Recent Res. Dev. Phys. Chem. 3 (1999) 133.
- [24] Y. Dimitrova, Recent Res. Dev. Phys. Chem. 6 (2002) 127.
- [25] Y. Dimitrova, J. Mol. Struct. (Theochem.) 668 (2004) 57.
- [26] J. Goebel, B.S. Ault, J. Phys. Chem. A 104 (2000) 2033.